JOURNAL OF CATALYSIS 44, 281–292 (1976)

Correlation between the Spectroscopic Properties of Iron Phthalocyanines and Their Activities for Electrodic Reduction of Oxygen in Alkaline Media

A. J. APPLEBY, J. FLEISCH,[1] AND M. SAVY

Laboratoire d'Electrolyse du C.N.R.S., 20 Place Aristide Briand, 92190 Meudon Bellevue, France

Received November 20, 1976

Specimens of iron phthalocyanines (polymer and monomer) were examined by optical and Mössbauer spectroscopy to identify the oxidation state, type of coordination, and spin configuration of the iron. Electrochemical measurements for oxygen reduction in alkaline solution carried out by the ultrathin electrode technique on suitably supported preparations showed that greatest activity occurred for fivefold coordinated Fe^{III} in the intermediate-spin state. The reaction mechanism was determined.

INTRODUCTION

A major interest of phthalocyanine compounds is the correlation between their structural characteristics and their electrocatalytic activity, in particular for reactions such as the electrolytic reduction of oxygen.

Manassen (*1*) determined the oxidation potentials and dehydrogenation reaction activities of phthalocyanines with differing central metal atoms and established a correlation as a function of atomic number or number of *d*-electrons of the latter, with a discrepancy for Zn and Cu. More recently (*2*), the activity for oxygen reduction was determined to be similar for Fe^{3+} and Fe^{2+} phthalocyanines, thus introducing a further discrepancy. Randin (*3*) gave evidence of correlation between oxidation potentials, magnetic moments, the rate of the cyclohexadiene/benzene dehydrogenation process, and the electroreduction of oxygen (*4*) for Cu, Ni, Co, and Fe phthalocyanines. Simple relationships were found.

[1] E. Zintl Institut, Technische Hochschule, 61 Darmstadt, Germany.

Savy *et al.* (*4*) and Alt *et al.* (*5*) attempted to explain the higher O_2 reduction activity of Fe and Co compounds by a model for O_2 adsorption using MO theory, as developed by Zerner *et al.* (*6*) for O_2 adsorption on porphyrins. According to this theory, oxygen radical formation is favored by formation of a dative double σ–π bond between molecular oxygen and the central ion. The O_2 molecule can receive an electron from the central ion via the π bond or release it via the σ bond and vice versa. This catalytic bond would then be favored (*5*) by filled d_{xz}, d_{yz} orbitals and empty d_{z^2} orbitals.

The effect of polymerization of the phthalocyanine has been investigated by Meier *et al.* (*7*). For Fe and Cu polyphthalocyanines synthesized under various conditions, polymerization results in an increase in electronic conductivity, accompanied by an increase in catalytic activity and stability. They interpreted these effects by supposing an increase in electron density at the central atoms of the polymer compared with that of the mono-

mer. According to the MO models proposed in (*4*) and (*5*), this should lead to enhanced electron exchange via π^{**} antibonding orbitals of the oxygen molecule.

The following special characteristics may be expected for polymeric phthalocyanines, compared with those for monomers: (i) In the absence of oxygen, there is an increase in *d* electron density at the central atom with increasing π electron density. The *d* electron density will decrease in the presence of oxygen due to electron trapping; (ii) reduction of oxidation potential; (iii) increase in magnetic moment; (iv) reduction of the O_2 molecule-central atom bond strength by injection of electrons into the π^* antibonding orbitals. Overall, the effect of polymerization should be to push the O_2 central atom bond strength closer to the optimum for effective catalysis [assuming an effect of the volcano type (*10*) holds] resulting in a lower free energy of activation for O_2^- formation and a more reversible oxygen reduction potential.

In previous work (*8*), it was found that the increase in the number of unpaired electrons detected by optical and ESCA spectroscopy was accompanied by an increase in the electrochemical activity for oxygen reduction on thin layers of phthalocyanine monomers in acid and alkaline solutions. However, the techniques used were unable to differentiate the activities of different lattice sites in terms of their oxidation state and spin configuration.

In this paper, such correlations have been conducted using a combination of optical reflectance spectrometry, Mössbauer spectrometry, and electrochemical experiments on monomeric and polymeric iron phthalocyanines prepared by gas- and liquid-phase methods (*8a, 8b, 9*). A certain number of experiments were performed on Eastman Kodak monomeric iron phthalocyanine, prepared by precipitation onto carbon black support from concentrated sulfuric acid solution (*9*). Blank experiments on the support were also conducted.

Where it is applicable, the use of Mössbauer spectroscopy permits determination of valency state and spin configuration of the iron in the bulk material. These parameters can also be determined by optical spectrometry and, in particular, the use of a combination of optical reflectance and transmission can establish differences in constitution between the electronic configurations of the bulk material and the outer monolayers.

To establish the reaction mechanism for oxygen reduction in alkaline solution on the polymeric phthalocyanine, two kinds of electrochemical measurements were conducted: (i) steady state measurements as a function of pH in the alkaline range and of oxygen partial pressure (apparatus, electrode preparation, and measurement techniques for these experiments have been described earlier, *8a, 8b, 9*); (ii) rotating disk ring electrode measurements to detect the presence of free intermediates (HO_2^- ion) produced in the reaction.

EXPERIMENTAL

Three types of iron phthalocyanine preparation were examined:[2] 1. Gold foils carried thin vacuum deposited films (*8*), corresponding to blue (electrochemically inactive) and green (electrochemically active) forms of the monomer (I_{c2} $I_{c'2}$, respectively, in the text below). The difference between the two forms resulted from the rate of vacuum deposition used. This was very rapid for the $I_{c'2}$ form (less than 1 sec) and slow (several minutes) in the case of I_{c2}.

2. Iron polyphthalocyanines and monophthalocyanines in 10% weight loading on acetylene black (Lannemezan Y) and active carbon (Norit BRX) supports: Preparation

[2] To avoid confusion, the following code is used in discussions: I = monomer; II = polymer; *a* = gas phase preparation; *b* = liquid phase preparation; *c*, *c'* of commercial origin; 0 = pure powder without support; 1, support on high surface carbon; 2, support on polished gold surfaces.

was as follows:

(a) The *in situ* gas phase technique was similar to that described earlier (*9*) using 1, 2, 4, 5 tetracyanobenzene and a volatile metal chelate (ferrocene or dipivaloylmethane). The preparation therefore differed significantly from that reported by Inoue *et al.* (*12a–c*) and Boston and Bailar (*13a*). In a typical preparation, 2.5 equivalents of the tetracyanobenzene and 1 equivalent of metal carrier were heated in a sealed tube at 250°C for 20 hr with the quantity of carbon support to give the required loading. The material was extracted with benzene in a Soxhlet for 2 hr, washed with alcohol and ether, and dried at 150°C under vacuum. These materials are designated type II_{a1} phthalocyanines.

(b) The method of Drinkar and Bailar (*14*) (type II_{b1} phthalocyanines): The material was prepared by liquid phase reaction of urea, pyromellitic dianhydride, and $FeCl_3$, washed, and dissolved in concentrated sulfuric acid. Specimens were prepared by dilution of a slurry of carbon support and phthalocyanine in sulfuric acid to give the required degree of impregnation.

(c) Pure monomer was prepared in liquid phase as in 2(b), but using phthalic anhydride instead of promellitic anhydride. This was supported on high-surface carbon (type I_{b1} phthalocyanine).

3. Pure monophthalocyanine powder of commercial origin (Eastman Kodak), designated type I_{c0}, together with pure gas phase monomer powder was prepared as in 2(a) using 1,2-dicyanobenzene (designated type I_{a0}), and pure liquid phase powder was prepared as in 2(c) (designated I_{b0}).

X-ray fluorescence data and N/Fe ratio determination (*8b*) have shown that the predominant species is a dimer in the case of gas phase preparation II_{a0}. Boston and Bailar (*13a*) have reported that the products of the liquid phase reaction using pyromellitic dianhydride are also polymeric phthalocyanines.

Mössbauer Spectra

The Mössbauer spectra were measured in transmission geometry using a constant acceleration electromagnetic drive operating in the multiscaling mode. The $^{57}Co/Cu$ source was kept at 293°K, whereas two absorber temperatures (293 and 77.4°K) were selected. The spectra were computer fitted to Lorentzian lines by least squares iterations.

Data were obtained for both monomeric and polymeric powders prepared by gas-phase synthesis (I_{a0} and II_{a0}). The absorber thickness was about 0.15 mg of $^{57}Fe/cm^2$ in this case.

In addition, thin layer monomers, similar to those used in the optical spectra experiments but this time deposited on mylar film, were examined. Twenty pieces of film were required to give a detectable spectrum with total iron equal to 0.065 mg of ^{57}Fe (blue specimen) and 0.032 mg of ^{57}Fe (green specimen). Spectra were recorded only at liquid nitrogen temperature.

The quadrupole splitting (Δ) is a function of the quadrupole moment of the nucleus Q and of the Electric Field Gradient which itself consists of two terms:

$$EFG = EFG_{\text{ligand-lattice}} + EFG_{\text{valence}}. \quad (1)$$

The first term corresponds to the effects of noncubic charge distribution and depends only on crystal structure: e.g., for square planar symmetry there is more ligand-lattice contribution than for octahedral symmetry. The second term involves nonspherical distribution of valence electrons in the valence shell.

Results obtained are summarized in terms of isomer shifts (δ) and Δ (concerning Mossbauer results) values in Table 1.

TABLE 1

Mössbauer Data[a]

	δ_1	$1/2\Delta_1$	δ_2	$1/2\Delta_2$	δ_3	$1/2\Delta_3$	δ_4	$1/2\Delta_4$	δ_5	$1/2\Delta_5$
Monomer (90)	0,18	A 56 1,16	0,16	B 15 0,54	0,12	C 23 0,23	0,01	D 5 1,62	-0,27	E 1 1,83
Monomer (298)	0,14	1,24	0,10	0,57	0,07	0,25	-0,02	1,76	0,39	1,09
Foil, blue (90)	0,16	A_1 45 1,13	-0,11	B_1 24 0,70	-0,03	C_1 29 0,23				
Foil, green (90)	0,24	A_1 43 1,22	-0,04	B_1 28 0,55	0,32	C_1 29 0,36				
	Triplet Fe^{2+}		or Fe^{3+} HS Fe^{2+} LS		Fe^{3+} green HS		Fe^{3+} LS			
	δ_1	$1/2\Delta_1$	δ_2	$1/2\Delta_2$	δ_3	$1/2\Delta_3$				
Polymer (298)	0,004	A_2 80 0,90	-0,10	B_2 15 1,35	0,44	C_2 5 0,66				
Polymer (90)	0,03	A_2 84 0,83	-0,06	B_2 12 1,24	0,26	C_2 4 0,49				
	Fe^{3+} IS		monomer Triplet Fe^{2+}		Fe^{3+} HS					

[a] Symbols used: δ: isomer shift mm-s^{-1}; Δ: quadrupole splitting mm-s^{-1}; $\boxed{\begin{matrix}A\\56\end{matrix}}$, $\boxed{\begin{matrix}B\\15\end{matrix}}$, $\boxed{\begin{matrix}C\\23\end{matrix}}$, . . . indicate the percentage of each form A, B, C, ... Figure after specimen is temperature (K).

Identification of the forms

Species present are indicated below, using the data given in Table 1.

Monomeric Powder (Gas Phase Synthesized) I_{a0}

Species A. The δ has a similar value to that reported by Dale (*16*). The Δ is slightly lower, but the difference is not significant. It can be assigned to Fe^{2+} with $S = 1$, ^3E being the ground state.

Species B. From literature data (*15*) the δ is not characteristic of Fe^{III} high spin (HS). However, it may correspond to Fe^{II} low spin (LS) though the Δ is too large for normal Fe^{II}LS.

Two possibilities exist for the larger QS value: either there is mixing of an excited state with the singlet, or there is a very large lattice contribution (Eq. 1). Large Δ values occur for both Fe^{2+} and Fe^{3+}, which result from low symmetry of the ligand field (*15*). $S = \frac{5}{2}$ is also possible (for $S = \frac{1}{2}$, a variation of Δ with temperature would be observed).

Species C. This species is similar to species B, however, the Δ value is lower, indicating a higher symmetry than for the latter. Since a peak characteristic of Fe^{III} (*8*) occurs in the optical spectrum, C must be Fe^{3+} HS, $S = \frac{5}{2}$.

Species D. This may be assigned to Fe^{3+} LS, $S = \frac{1}{2}$, since δ is near zero and the Δ value is temperature-dependent.

Thin Film Monomers

Mössbauer characteristics of Eastman Kodak and gas phase-synthesized monomers (I_{a2}, I_{c2}, $I_{c'2}$) in the form of thin films were similar.

The main species (A_1) in both cases is monomeric Pc Fe^{II} with almost the same δ and Δ values as those for the original powder. Species B_1 presents a lower δ than the B species in the powder.

The principal difference between the two films involves a resonance peak which corresponds to Fe^{3+} HS, $S = \frac{5}{2}$ or $S = \frac{3}{2}$, as determined by the δ and Δ values. Species C_1 is observable in the green film. This result is in agreement with the interpretation of optical ESCA data given previously (*8*).

In both films, the resonance lines of species B_1 and C_1 are stronger than for the monomeric powder, corresponding to some oxidation of Fe^{II} to Fe^{III} during vacuum sublimation. This effect is more pronounced with the green film.

Polymers II_{a0}

Species A_2. δ and Δ values (*15*) which coincide with those determined experimentally are for Fe^{3+} in intermediate spin configuration (IS) within a fivefold-coordinated ligand. The Δ is too large for a sixfold-coordination. A higher Δ value occurs than that for species C of the monomer, indicating a lower symmetry.

This identification is in accord with the optical reflectance spectra (see below) obtained on monomeric powder (I_{c0} and I_{a0}) II_{a0} synthesized powder and a polymeric II_{b0} prepared powder. It can be assigned to be Fe^{3+} HS from the position of the absorption peak.

Species B_2. Δ values are very close to those of species A in the monomeric powder. The δ value is lower for both A_2 and B_2 than that of the corresponding species A and B in the monomer. This may be accounted for by the decreased *d* electron density of the central iron. The values of δ and Δ preclude an electronic configuration similar to those of species B and C of the monomer.

Species C_2. For all parameters of this species, experimental errors are relatively large, because of the small area of the resonance lines. From the δ value, it can be identified as Fe^{3+}.

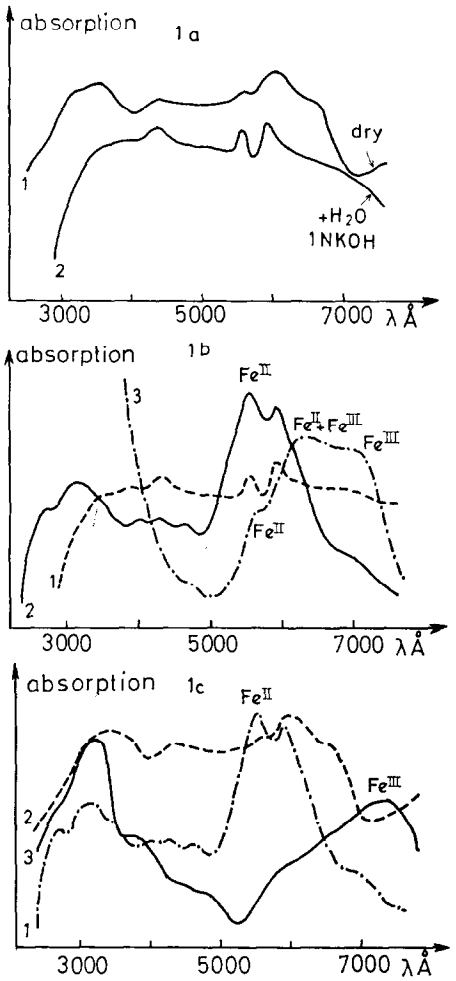

FIG. 1. Optical reflection spectra for phthalocyanines. (a) Polymer gas phase preparation (reflection): (1) air, (2) 1 *N* KOH. (b) Monomer Eastman and gas phase preparation: (1) 1 *N* KOH (reflection), (2) air (reflection), (3) thin layer active form (transmission). (c) Monomer and polymer in air (reflection): (1) monomer Eastman and gas phase preparation, (2) polymer gas phase preparation, (3) polymer liquid phase preparation.

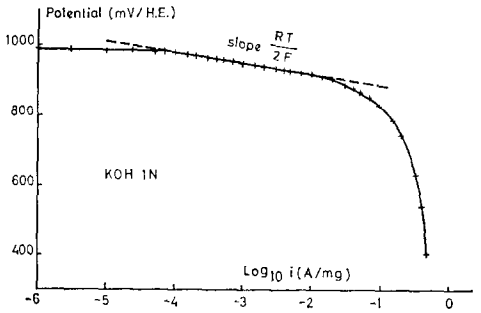

FIG. 2. Oxygen reduction in KOH on gas-phase iron polyphthalocyanine (10% by weight on acetylene black).

The Δ value corresponds to a HS configuration. It should be noted that the ratio of the Fe^{3+} HS/Fe^{2+} triplet is approximately the same as that for the monomer.

Optical Spectroscopy

Spectra (transmission spectra in the case of the thin films, reflection spectra for the supported or unsupported powders) were obtained in the dry state and in the presence of 1 N KOH solution, both in the presence of air, using a Cary 17 spectrometer. They are shown in Fig. 1. Spectral changes showing the effect of wetting the II_{a0} preparation with KOH are shown in Fig. 1a, curves 1 and 2. On wetting, only two peaks can be detected, which are identical for all forms of the phthalocyanines examined (curve 1, Fig. 1b). The emission in the uv results from fluorescence.

Curve 2 in Fig. 1b represents the reflection spectrum obtained on the monomeric form I_{a0} powder. The position of the two main peaks on this curve shows them to be the same as the two similar peaks of curve 1. They are characteristic (see below) of Fe^{II} triplet state.

After drying in air at room temperature, the spectra become identical to those obtained before wetting. Since a transformation involving the bulk material is unlikely to be reversible and can in any case be excluded for reflectance spectral data, wetting results in modification of the oxidation state and the spin configuration of the outer monolayers. Curve 3 in Fig. 1b represents the spectrum obtained by transmission through the films (I_{a2}, I_{c2}). It is apparent that several different forms are present.

Reflection spectra for unsupported powders (I_{c0}, I_{b0}, II_{a0}, and II_{b0}) are given in Fig. 2c. Spectra for both monomeric forms are identical. A shift of the main absorption peaks to longer wavelengths is observed in the order:

$$II_{b0} > II_{a0} > I_{a0}, I_{c0}.$$

From ESCA data (*8*), the position of the main absorption peak of the II_{a0} preparation corresponds to the Fe^{3+} HS and the monomer to Fe^{2+} intermediate spin (IS). As the shift to longer wavelength increases with the spin (*8*), this indicates the presence of either Fe^{2+} HS or Fe^{3+} IS in the II_{a0} preparation, so that the inequalities for wavelengths:

$$Fe^{3+}HS(\tfrac{5}{2}) > Fe^{2+}HS(2), Fe^{3+}IS(\tfrac{3}{2}) > Fe^{2+}IS \quad (1)$$

are satisfied.

Electrochemical Measurements

Steady State Results

Steady state measurements were performed on ultrathin porous diffusion electrodes of the type first described by Vogel and Lundquist (*17*). The electrodes, which consist of a Teflon-bonded layer less than five catalyst particles thick, allow pure kinetic measurements to be made on finely powdered electrode materials without diffusion limitations (*9*).

Rest Potentials, Tafel Slopes

When examined by the ultrathin electrode techniques (*9*) with catalyst weights in the 0.1 mg/cm² range, Tafel plots of slope equal to 30 mV/decade at 25.0°C

were obtained over a 2–3 decade range of current density. A plot in N KOH solution at 1 atm O_2 is given in Fig. 2.

Similar Tafel slopes were obtained over a wide pH range. No hysteresis was observed and reproducibility was to within 2–3 mV for different electrodes. Rest potentials varied between 990–983 mV vs hydrogen in the same solution throughout the pH range studied (see below).

Effect of Oxygen Partial Pressure

Results were obtained over a range of oxygen partial pressure varying from 5×10^{-3} atm to 1 atm. Log current density at a constant potential in the Tafel region, at 925 mV (hydrogen), is plotted in Fig. 3 as a function of log O_2 partial pressure. The slope of the straight line obtained is 1.08. We can therefore presume a first-order reduction of oxygen.

Effect of pH

Polarization-current density results were obtained in 1 N K_2CO_3, pH 11.80; 1 N K_2CO_3/KOH buffer, pH 13.0; 1 N KOH, pH 13.90; and a series of KOH solutions varying from 2 N to 12 N concentration (pH 14.2 to 16.4). pH values for the latter were calculated from activity coefficient values given in Ref. (*18*). Activity in the Tafel region, if necessary extrapolated, at a constant current density, is shown in Table 2.

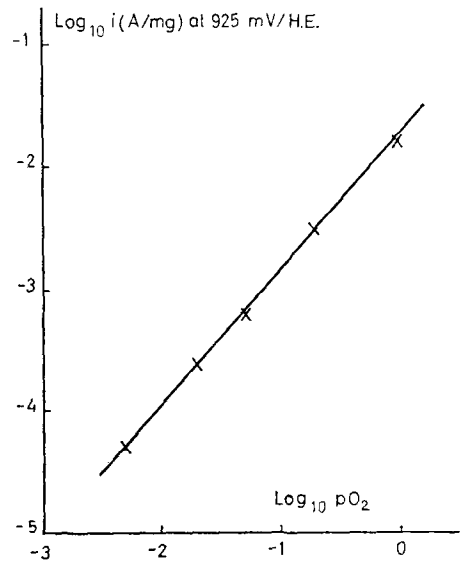

FIG. 3. Log–Log plot of current at +925 mV/HE as a function of pO_2 (2 N KOH). Slope = +1.08.

TABLE 2

Potential at a Current Density of 10^{-3} A/mg

Solution	pH	Potential vs hydrogen (mV)
1 N K_2CO_3	11.8	955
N K_2CO_3–KOH	13.0	955
1 N KOH	13.9	955
2 N KOH	14.2	957
4 N KOH	14.75	960
6 N KOH	15.2	960
9 N KOH	15.8	955
12 N KOH	16.4	960

Oxygen Reduction on Carbon Black Support and Monomeric Iron Phthalocyanine

Results obtained in 6 N KOH at 25°C are shown in Fig. 4. It is evident that the polymeric phthalocyanine confers activity much greater than that of the support in the non-diffusion-limited region. In contrast, the effect of the monomer (Eastman Kodak, 10% by weight prepared from concentrated H_2SO_4 solution) is to mask the intrinsic support activity, at least in the diffusion region. Oxygen reduction on a liquid phase polymer preparation is also shown. Its activity is less than that of the gas-phase preparation.

Ring-Disk Electrode Experiments

A ring-disk electrode (Tacussel) with a cavity shaped in the gold disk was used (*19*). The ring was gold with a gold-black electrodeposit. The iron polyphthalocyanine on carbon black support was introduced into the cavity in the form of a paste

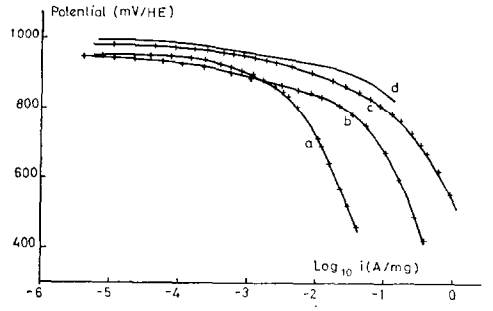

FIG. 4. Oxygen reduction in 6 *N* KOH. (a) On monomer Fe phthalocyanine (10% by weight on acetylene black); (b) on support; (c) on polymer, liquid-phase preparation (10% by weight on acetylene black); (d) on gas-phase polymer preparation.

incorporating purified mineral oil (*19*), followed by accurate smoothing of the surface.

Collection efficiency of the electrode was determined to be 0.17 in a redox solution. In contrast to previous work on carbon blacks (*18*), no hydrogen peroxide was detected at potentials above 600 mV vs hydrogen in the pH range 11,8–16.4, though small quantities were noted at higher polarizations. At each pH, the half-wave potential was independent of rotation rate indicating no diffusion control by a soluble reaction product.

Oxygen reduction on the iron polyphthalocyanine is, for potentials above 600 mV, a 4-electron process not involving hydrogen peroxide as detectable intermediate.

Determination of the chemical order of reaction for OH^- presents some difficulty, since O_2 solubility (*20a, b*) and H_2O activity simultaneously change with increasing concentration of KOH. A reduction by a factor of 30 and 4 occurs for $[O_2]$ and $[H_2O]$ between 1 *N* and 12 *N* KOH (*20a, b, 21*) respectively.

A complete analysis (*22*) of the pH dependence data indicates an apparent chemical reaction order for $[OH^-]$ equal to -1.67 assuming zero order in H_2O. However, a zero order in H_2O is physically improbable. Since each OH^- generated before the rate determining step will require one molecule of water, the reaction must have, at least, the same positive order in H_2O as it has negative order in OH^-. It may, for example, have an order of $+2$ in H_2O (H_2O involved in the rate determining step and a preceding step, yielding OH^- as product) and -1 in OH^-. Since the apparent order determined (assuming a constant H_2O concentration) is less than -2 in OH^-, then it is reasonable to suppose an order of either $+1$ or $+2$ in H_2O. Calculation (*22*) shows a true order in OH^- of -1.43 and 1.19, respectively, for postulated H_2O orders of $+1$ and $+2$ using the values for the variation in water activity in reference (*21*) in the solution considered. An H_2O order of $+2$ and an OH^- order of -1 therefore seem closest to the experimental results observed.

DISCUSSION

Reaction Mechanism on Polyphthalocyanines

The reaction has been determined to be first order in O_2, and apparently of order of -1 in OH^-. An order of a least $+1$ for water is probable. The Tafel slope is very low, about 30 mV/decade (RT/2F), the value of α defined as in Ref. (*23*) being close to 2.0. The reaction is not controlled by diffusion of a dilute product, as shown by the ring-disk electrode data. α is given by the expression (*23*):

$$\alpha = \frac{n}{\nu} + \beta n', \qquad (2)$$

where n is the number of electrons reversibly transferred before the rate determining step, whose symmetry factor is β and whose stoichiometric number is ν (the number of rate determining step units for each unit overall process). We can exclude n' values other than 0 and 1 (*24*). β will normally be close to 0.5 for metallic conductors under Langmuir adsorption conditions but may have an effective value

of 1 under certain conditions (e.g., Temkin type adsorption of reaction intermediates on metallic surfaces (*25*) or under normal charge transfer conditions at relatively thick wide-gap semiconductors (*26*).

With $\alpha = 2$, possible values of n/ν are:

$$n/\nu = 2; \quad \beta = 0.5 \text{ or } 1; \quad n' = 0$$
$$n/\nu = 1; \quad \beta = 1; \quad n' = 1.$$

That is, the rate determining process is either a chemical step after two rapid electron transfer steps, or an electrochemical step with $\beta = 1$, following a rapid electron transfer step. Steps with, for example, $\nu = 2$ can be discounted because they imply a dissociation step giving two identical products, which then react separately in two similar unit rate determining steps resulting in a reaction order for molecular oxygen equal to 0.5.

In consequence, we suggest the following possible processes:

$$O_2 \rightarrow O_{2ads} \quad \text{(rapid)} \quad \text{I}$$

$$O_{2ads} + H_2O + e^- \rightarrow HO_{2ads} + OH^- \quad \text{(rapid)} \quad \text{II}$$

$$O_2H + H_2O + e^- \rightarrow H_2O_2 + OH^- \quad \text{III}$$

$$H_2O_2 \rightarrow 2OH \quad \text{IV}$$

in which either step III or IV is rate determining. If step III is rate determining, an effective β value of 1.0 is implied, resulting from a directly field-dependent charge carrier concentration. Since the semiconducting polyphthalocyanine layer is very thin (about 20 Å), a high charge carrier density is implied in this case. However, for the reasons stated below, we feel that charge transfer is likely to be rapid with these compounds. A rate determining chemical step is therefore more probable. Since H_2O_{2ads} in step III is not likely in strongly alkaline solution, we feel that the most probable process will be I and II above followed by:

$$HO_{2ads} + e^- \rightarrow HO_2^-{}_{ads} \quad \text{(rapid)} \quad \text{V}$$

$$HO_2^-{}_{ads} + H_2O \rightarrow 2OH + OH^- \quad \text{(rate determining)} \quad \text{VI}$$

$$OH + e \rightarrow OH^- \quad \text{(fast)} \quad \text{VII}$$

A slow chemical step involving breaking of the O–O bond is therefore most probable. This mechanism is in agreement with the electrochemical and reaction order data, but more work is necessary before it can be definitely established.

Correlation with the Spectroscopic Data

Comparing the experimental data with those already published (*9*), the electrochemical activities of the samples investigated may be placed in the order:

$$\text{Polymer II}_{a1} > \text{Polymer II}_{b1} > I_{a2}; I_{c2} \gg I_{a1}; I_{b1}; I_{c1}.$$

For the most active samples II_{a1} in the dry state, Fe^{III} IS was detected as the main iron species by both Mössbauer and reflection spectra. On the other hand, the less active samples consist predominantly of Fe^{II} in the triplet state. For monomers on foils, activity increases with the relative concentration of $Fe^{III}HS$ detected by Mössbauer and optical transmission spectra. The activity of the material on foil support (I_{a2}; I_{c2}) is less than that of II_{b1}, which consists mainly of $Fe^{III}HS$. From the relative concentrations of the different Fe species, their activities may be put in the order:

$$Fe^{III}IS > Fe^{III}HS > (Fe^{III}HS, Fe^{III}IS) \gg Fe^{II}IS.$$

It must be emphasized that the relative concentration of the Fe species is strongly dependent upon the sample preparation procedure. This result is in accordance with the findings of Baker *et al.* (*13b*) concerning cyclohexene oxidation and their lack of agreement with the results of Inoue *et al.* (*12*). It may also account for the larger quantities of H_2O_2 detected by Tarasevich and Bogdanovskaya (*27*)

on a monomer preparation compared with those reported here.

In the presence of KOH and oxygen, reflectance spectral data show that the interface corresponds to a low activity form (Fe^{II} in the triplet state), while for the optical transmission spectra the position of the peaks remains unaffected. The other change noted is a slight modification of the adsorption coefficient. The difference in structure between the surface and the bulk of the material investigated seems likely to modify the kinetics of oxygen reduction since in step I an increase of the amount of adsorbed oxygen involved in the electrochemical reaction will occur with an increase of $Fe^{III}HS$ or $Fe^{III}IS$.

The appearance of Fe^{III} in the polymeric materials may be either due to an increase of π electron density in the conjugated rings in the presence of oxygen or may result from trapping of the *d*-electrons by bonded oxygen, implying a π electron displacement toward the central ion with localization on the bonded oxygen. For the latter explanation, following the model given by Zerner *et al.* (*6*) for porphyrins, increased electron donation to the oxygen should occur, the latter being more ionized than in the case of the monomer. This implies a lower bond strength (increased lability) since electrons are added to the antibonding levels of oxygen. Further Mössbauer experiments in the absence of oxygen may bring support for a choice between these two hypotheses.

In accordance with the data obtained, the following initial reaction path can be proposed (i.e., corresponding to steps I and II above). A chemisorption step activated by the iron spin configuration (Fe^{II}–O_2 HS or IS) in the bulk material, i.e.:

$$O_2 + PPcFe^{III}\text{–}O_2^- \rightleftarrows O_2{*}PPcFe^{III}\text{–}O_2^- \quad \text{VIII}$$

followed at the interface by

$$PPcFe^{III}\text{–}O_2^- + H_2O \rightarrow PPcFe^{II}O_2H + OH \quad \text{IX}$$

$$OH + e \rightarrow OH^-$$

corresponding to step II followed by steps V, VI, and VII at the catalyst-solution interface.

The higher $Fe^{III}IS$ concentration may also act on step VI. The OH radical produced can either be reduced to OH^- or enhance the chemical r.d.s. by the sequence of reactions:

$$HO_2^- + OH \rightarrow OH^- + HO_2 \quad \text{VI-1}$$

$$HO_2 + HO_{2\,ads} \rightarrow 2OH + O_2 \quad \text{VI-2}$$

in which all the species involved can react together either by nonsequential coupled chemical or fast electrochemical reactions such as II, V, and VII.

Action on Electron Transfer Steps

Because electron transfer involves adsorption-desorption processes at the interface, higher *d*-electron density during the desorption step (inducing Fe^{III} formation) will also result in an increased overlap between acceptor and donor levels giving higher electron transfer rates. This is in accord with the presence of a chemical r.d.s. in the oxygen reduction mechanism.

Assuming electron transfer is occurring through excited states of the form:

$$HS\,(d_{xy})^1(d_{xz,yz})^2(d_{z^2})^1(d_{x^2-y^2})^1 \rightarrow (d_{xy})^0(d_{yz,xz})^3(d_{z^2})^1(d_{x^2-y^2})^1 \quad \text{X}$$

$$IS\,(d_{xy})^2(d_{xz,yz})^2(d_{z^2})^1(d_{x^2-y^2})^0 \rightarrow (d_{xy})^1(d_{yz,xz})^3(d_{z^2})(d_{x^2-y^2})^0, \quad \text{XI}$$

the probability π for electron transfer can be written as:

$$\pi HS \sim |\langle \psi_g{}^6 | \hat{0}_\rho | \psi_{ex}{}^4 \rangle|^2 > 0 \quad (4)$$

$$\pi IS \sim |\langle \psi_g{}^4 | \hat{0}_\rho | \psi_{ex}{}^4 \rangle|^2 > 0, \quad (5)$$

where ψ is the wave function of the ground state sexet in the HS form or of the quartet in the IS form. ψ_{ex} is the wave function of the excited state quartet in both cases. $\hat{0}_\rho$ is the exchange integral which does not act on the spin. It is clear that processes involving no change of spin (e.g., πIS) are much more likely to be adiabatic.

CONCLUSION

Previous models using MO theory as developed by Zerner *et al.* (*6*) indicate that the optimum suitable electronic configuration for the electrosorption of oxygen is d^5 in the IS or HS state. Experimental support of these conclusions is given by Mössbauer and optical reflectance spectroscopy on monomeric and polymeric powder samples, together with electrochemical data, to determine the reaction mechanism for oxygen reduction in alkaline solution.

While reduction of oxygen on monomeric material is relatively slow, an increase of activity by more than one order of magnitude is observed on polymeric samples. Mössbauer and optical reflectance spectroscopy indicate that this increase in activity corresponds to an increase of the Fe^{III} sites in the HS or IS configuration. A 4-electron reduction process occurs on the polymer, indicating an increase of the electron transfer rate in parallel with an increase in the oxygen chemisorption rate. The most probable rate determining step is the breaking of the O–O bond.

Since optical reflectance spectra in the presence of KOH are similar for monomer and polymer ($Fe^{II}IS$) (optical transmission spectra remaining unchanged), we suggest that chemisorption initially occurs inside the bulk of the catalyst, the oxygenated radicals diffusing thereafter to the interface. This is in agreement with previous work showing an increase in activity with thickness for monomer films, for which adsorption is rate determining (*8*). The effect of polymerization on activity can be interpreted by an increased *d*-electron density due to the conjugated rings. Simultaneously oxygen chemisorption and electron transfer are enhanced.

ACKNOWLEDGMENTS

We wish to thank G. Magner for the optical spectroscopic measurements, G. Crepy for the electrochemical measurements, and the Deutsche-forschungsgemeinschaft for a grant to one of us (M. S.).

REFERENCES

1. Manassen, J., and Bar Ilan, A., *J. Catal.* **17**, 86 (1970).

2. Manassen, J., *J. Catal.* **33**, 133 (1974).

3. Randin, J. P., *Electrochim. Acta* **19**, 83 (1974).

4. Savy, M., Andro, P., Bernard, C., and Magner, G., *Electrochim. Acta* **18**, 191 (1973).

5. Alt, H., Binder, H., and Sandstede, G., *J. Catal.* **28**, 8 (1973).

6. Zerner, M., Gouterman, M., and Kolayashi, H., *Theor. Chim. Acta* **6**, 363 (1966).

7. Meier, H., Albrecht, W., Tchirwitz U., and Zimmerhackl, E., *Ber. Bunsengs. Phys. Chem.* **77**, 843 (1973).

8a. Savy, M., Bernard, C., and Magner, G., *Electrochim. Acta* **20**, 383 (1975).

8b. Savy, M., Andro, P., and Bernard, C., *Electrochim. Acta* **19**, 403 (1974).

9. Appleby, A. J., and Savy, M., *Electrochim. Acta* **21**, 567 (1976).

10. Balandin, A. A., "The Problems of Chemical Kinetics, Catalysis and Reactivity," p. 462. Acad. Sci. of the USSR, Moscow, 1955.

12a. Inoue, H., Kida, Y., and Imoto, E., *Bull. Chem. Soc. Jap.* **38**, 2214 (1965).

12b. Inoue, H., Kida, Y., and Imoto, E., *Bull. Chem. Soc. Jap.* **40**, 184 (1967).

12c. Inoue, H., Kida, Y., and Imoto, E., *Bull. Chem. Soc. Jap.* **41**, 684 (1968).

12d. Inoue, H., Kida, Y., and Imoto, E., *Bull. Chem. Soc. Jap.* **41**, 692 (1968).

13a. Boston, D. R., and Bailar, J. C., *Inorg. Chem.* **11**, 1578 (1972).

13b. Baker, D. J., Boston, D. R., and Bailar, J. C., *J. Inorg. Nucl. Chem.* **35**, 153 (1973).

14. Drinkar, W. C., and Bailar, J. C., *J. Chem. Soc.* **81**, 4795 (1959).

15. Greenwood, N. N., and Gibb, T. C., "Mössbauer Spectroscopy." Chapman and Hall, London, 1971.

16. Dale, B. W., and Williams, R. J. P., *J. Chem. Phys.* **498**, 3445 (1968).

17. Vogel, W. M., and Lundquist, J. L., *J. Electrochem. Soc.* **117**, 1512 (1970).

18. "Sprovochnik Khimiya," Vol. 3, p. 595, Khimiya, Moscow, 1964.

19. Appel, M., Thesis, Conservatoire National des Arts et Métiers, Paris (1974).

20a. Gubbins, K., and Walker, R., *J. Electrochem. Soc.* **112**, 469 (1965).

20b. Davis, R., Horvath, G., and Tobias, C., *Electrochim. Acta* **12**, 287 (1967).

21. Bro, P., and Kang, H. Y., *J. Electrochem. Soc.* **118**, 1430 (1971).

22. Appleby, A. J., and Savy, M., *Electrochim. Acta* (to be published).

23. Parsons, R. (cf. T. P. Hoar), "Proc. 8th Meeting CITCE," Madrid (1956), p. 439. Butterworths, London, 1958.

24. Vorotyntsev, M. A., and Kuznetsov, A. M., *Electrokhimiya* 6, 208 (1970).

25. Damjanovic, A., and Brusic, V., *Electrochim. Acta* 12, 615 (1967).

26. Green, M., "Modern Aspects of Electrochemistry," (J. O. M. Bockris, Ed.), Vol. 2, p. 343. Butterworths, London, 1959.

27. Tarasevich, M. R., and Bogdanovskaya, V. A., *Bioelectrochem. Bioenerget.* 2, 69 (1975).